Original Research

Regional Differences of fMR Signal Changes Induced by Hyperventilation: Comparison Between SE-EPI and GE-EPI at 3-T

Shinji Naganawa, MD,[1]* David G. Norris, PhD,[2] Stefan Zysset, PhD,[2] and Toralf Mildner, PhD[2]

Purpose: To evaluate whether reproducible signal change of brain tissues by hyperventilation (HV) can be seen on spin-echo (SE)-echo planar imaging (EPI) at 3-T and to examine the sensitivity of SE-EPI for measuring vascular reactivity in regions of the brain, such as the hippocampal formation, that are difficult to visualize with gradient-echo (GE)-EPI due to susceptibility artifacts.

Materials and Methods: Six healthy human subjects performed a voluntary HV task. The task design was as follows: two minutes normal breathing (rest) followed by two minutes HV, giving a basic four-minute block that was repeated three times for a total scan time of 12 minutes for one run. Each subject performed the run both for SE-EPI and GE-EPI. Statistical analysis was performed to detect the area with significant cerebrovascular reactivity. The percentage signal change was also obtained for each cerebral region.

Results: Both GE-EPI and SE-EPI showed globally significant signal decreases in the cerebral cortex. In GE-EPI, the frontal cortex showed a larger signal decrease than the other gray matter tissues ($P < 0.05$). In SE-EPI, the differences among gray matter tissues except for the hippocampal formation were not significant. The hippocampal formation showed the largest signal change ($P < 0.05$) in SE-EPI, but no significant signal change was observed in GE-EPI due to the presence of susceptibility artifacts.

Conclusion: HV using SE-EPI at 3-T provides robust and reproducible signal decreases and may make the evaluation of the vascular reactivity in hippocampal formation feasible.

Key Words: hyperventilation; functional; magnetic resonance; spin-echo; gradient-echo; vascular reactivity
J. Magn. Reson. Imaging 2002;15:23–30.

HYPERVENTILATION (HV) HAS PREVIOUSLY been used as an easy and reliable task for the assessment of global cerebral vascular reactivity (1–3). It is reported that the functional magnetic resonance (fMR) signal change induced by HV differs between cerebral regions (4). Signal changes are reported to be larger in frontal cortex than in cerebral white matter, cerebellum, and visual cortex (4). Frontal lobe dominance in vascular reactivity has also been reported using Xe-133 (5). This regional variability is at odds with the results reported for hypercapnia induced by breath-holding (6). These authors reported that signal change by breath-holding was larger in the cerebellum and visual cortex than in the frontal cortex. They speculated that regional differences in vascular reactivity were induced by differences in capillary density between cerebral regions, although the cause of discrepancies between the studies using hypo- and hypercapnia is unknown. Although spin-echo (SE) echo planar imaging (EPI) gives a lower blood oxygenation level-dependent (BOLD) signal change compared to gradient-echo (GE)-EPI, the two methods have different sensitivities to various vascular structures (7,8). The BOLD signal change detected by GE is mainly the result of static dephasing, which at 1.5-T is thought to mostly stem from the intravascular component in large veins (9,10), although the true origin of fMR imaging signal change still remains controversial (11). At 1.5-T using standard spatial resolution, the SE-EPI BOLD signal change is also mainly intravascular (12). However, at 9.4-T, the BOLD signal change detected by SE-EPI is independent of the intravascular component (13). At 3-T, it can reasonably be expected that the contribution from the intravascular component to SE-EPI BOLD signal change is lower compared to that at 1.5-T.

We conducted this study to evaluate whether reproducible signal change by HV can be seen on SE-EPI and to investigate whether this frontal dominance in vascular reactivity is seen on SE-EPI, as well as GE-EPI at 3-T. A further aim was to examine the sensitivity of SE-EPI for measuring vascular reactivity in regions of the brain, such as the hippocampal formation, that are difficult to visualize with GE-EPI due to susceptibility artifacts.

[1]Department of Radiology, Nagoya University School of Medicine, Nagoya, Japan.
[2]Max Planck Institute of Cognitive Neuroscience, Leipzig, Germany.
This work was performed while the first author was on leave from Nagoya University at the Max-Planck-Institute of Cognitive Neuroscience.
*Address reprint requests to S.N., Department of Radiology, Nagoya University School of Medicine, 65 Tsurumai-cho, Shouwa-ku, Nagoya, 466-8550 Japan. E-mail: naganawa@med.nagoya-u.ac.jp
Received July 2, 2001; Accepted August 27, 2001.

DOI 10.1002/jmri.10028

MATERIALS AND METHODS

Subjects

Six right-handed healthy subjects (three men and three women; 22–29 years old, average 25.8 years old) were included in this study. All subjects gave their written informed consent to participate in this study. This investigation was approved by the Ethics Committee of the University of Leipzig.

MR Imaging

All MR imaging was performed on a 3-T whole body MR scanner (MedSpec 30/100; Bruker Medizintechnik, Ettlingen, Germany) using a bird-cage head coil. Each subject's head was fixed tightly with foam pad packing. After the scout scan, anatomical T_1-weighted two-dimensional modified driven equilibrium Fourier transform (MDEFT) images (14) (256 × 256, TR 1.3 seconds, echo time [TE] of 10 msec) were obtained with a non-slice-selective inversion pulse followed by a single excitation of each slice (15). Slice orientation was made parallel to the bicommissural plane (AC-PC). For the registration purposes of EPI fMR images, a set of T_1-weighted inversion recovery EPI images was also taken with the same parameters as the fMR imaging data. The inversion time was 1200 msec, with a TR of 45 seconds and four averages. For each subject, high resolution whole-head T_1-weighted three-dimensional MDEFT images (16) were obtained with 128 sagittal slices, 1.5 mm thickness, field of view (FOV) of 25 × 25 × 19 cm, and 256 × 256 matrix for subsequent image registration. The three-dimensional MDEFT images were obtained in a different session to reduce total examination time. fMR imaging was performed using both single-shot GE-EPI and single-shot SE-EPI. For both sequences, the following parameters were employed: TR two seconds, 5 mm slice thickness, 2 mm gap, 64 × 64 matrix, FOV of 19.2 cm (in-plane resolution of 3 mm × 3 mm), 16 slices parallel to the AC-PC line, and bandwidth of 100 kHz. For GE-EPI, the flip angle was 90° and TE was 30 msec. For SE-EPI, a TE of 80 msec was used. The echo times chosen were appropriate for the expected relaxation times at 3-T.

HV Experiment

Subjects were instructed to perform voluntary HV for two minutes upon request by the operator. Subjects were also instructed to keep their heads as still as possible during HV. End-tidal CO_2 partial pressure ($EtCO_2$) was monitored via a nasal canula (three meters long) every three seconds using a "Maglife" capnometer (Bruker Medizintechnik, Ettlingen, Germany). The $EtCO_2$ measurement delay was approximately six seconds after expiration due to the dead space of the cannula.

The task design for HV was as follows: two minutes of normal breathing (rest) followed by two minutes HV, giving a basic four-minute block that was repeated three times for a total scan time of 12 minutes for one run.

Each subject was asked to perform the run both for SE-EPI and GE-EPI. Between the two runs, at least 10 minutes of rest period was set. The order of SE-EPI and GE-EPI was randomized in order to eliminate any systematic differences in response to repeated HV. SE-EPI was performed first in three subjects and GE-EPI was performed first in the other three subjects.

Data Analysis

Prior to the statistical analysis, individual subject's fMR data were visually inspected to check for gross motion and then preprocessed as follows: using an in-plane motion correction, baseline fluctuation was corrected for by using a voxel-wise high-pass filter in the temporal domain (cut-off period of 1.5 times of trial length), a spatial Gaussian filter, and a slice-time correction that linearly compensated for the time difference between slices. A transformation matrix was calculated by mapping the two-dimensional anatomical slices (two-dimensional MDEFT) onto the individual three-dimensional anatomical data set (three-dimensional MDEFT). For this purpose, a rigid linear registration with six degrees of freedom (three rotational, three translational) was performed. The rotational and translational parameters were acquired on the basis of the two-dimensional MDEFT to achieve an optimal match between these slices and the individual three-dimensional MDEFT reference data set. The inversion recovery EPI data was applied to refine the transformation matrix for fMR imaging by EPI. The statistical evaluation was based on a least-squares estimation using the general linear model for serially autocorrelated observations (17). First, for each individual subject, statistical parametric maps were generated and were averaged over all subjects afterwards (18). The design matrix was generated with a boxcar (square wave). The model equation, including the observation data, the design matrix, and the error term, was convolved with a Gaussian kernel of dispersion of four seconds full width half maximum (FWHM). The model included an estimate of temporal autocorrelation used to estimate the effective degrees of freedom. The contrast between the different conditions was calculated using the *t*-statistic. Subsequently, t-values were transformed to *z*-scores. As the individual functional datasets were all aligned to the same stereotactic reference space (19) by a linear affine transformation, a group analysis of fMR imaging data was performed by averaging individual *z*-maps and multiplying each *z*-value with square root of N (N = number of subjects) (18). During this process, data were linearly interpolated to 3 mm × 3 mm × 3 mm resolution. Regions with a *z*-score higher than 3.5 ($P < 0.0001$) were considered as responding significantly to HV. The *z*-maps and percentage signal changes were evaluated using the data from the last minute of each rest and HV period, to exclude the transient period between HV and rest. The percentage signal change from each brain region was measured in two ways. In one method, we chose a most significantly activated voxel in a particular region on the averaged normalized three-dimensional *z*-map of GE-EPI, and signal intensity values of a voxel and its neighboring 26 voxels were averaged in normalized three-dimensional space for the individual subject. By this method, a 729 mm^3 cubic volume was

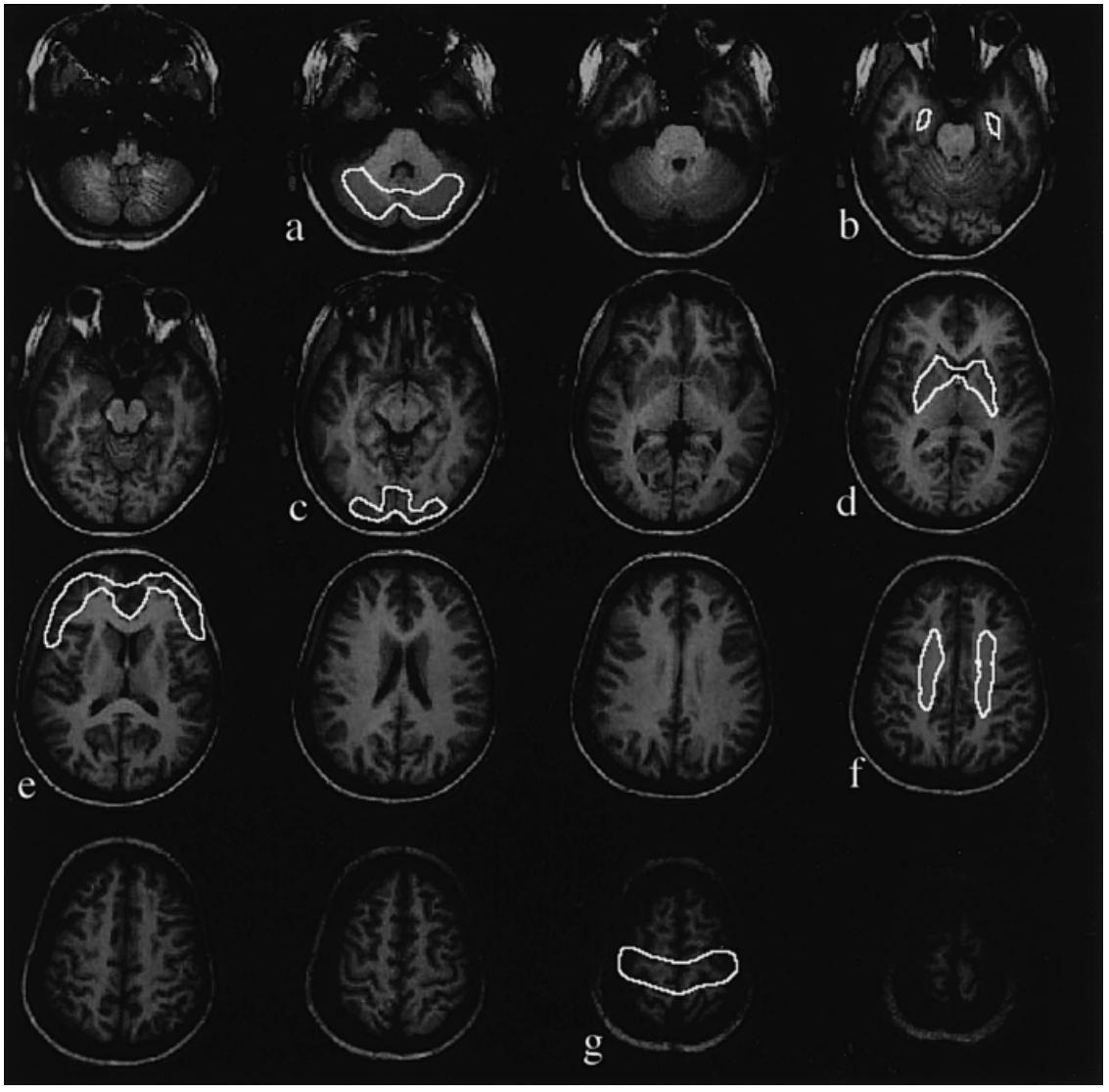

Figure 1. Axial T_1-weighted images showing the delineation of the larger ROIs. **a:** cerebellum, **b:** hippocampal formation, **c:** occipital cortex, **d:** basal ganglia, **e:** frontal cortex, **f:** white matter, **g:** parietal cortex.

evaluated. This measurement was performed for the frontal cortex, parietal cortex, occipital cortex, basal ganglia, hippocampal formation, cerebellum, and white matter. Each measurement was conducted for both hemispheres of the brain and an average from both sides was obtained. For each subject, the voxel with the same coordinate value in the normalized space was selected. Besides this relatively small region of interest (ROI) analysis, the second method used the larger ROIs drawn manually on two-dimensional non-preprocessed source images (raw data) for seven anatomical areas described above (Fig. 1). The percentage signal change in each ROI was also measured by this manual method. We used two kinds of ROI analysis methods because the smaller ROIs placed in significantly activated voxels might be more influenced by flow (20). However, although manually set larger ROIs might be more vulnerable to anatomical bias, we felt it worthwhile to evaluate non-preprocessed data to reduce the influence from the vessel itself and to exclude the possibility that one of the preprocessing methods could subtly modify the results of a small signal change. The average of three rest periods and three HV periods were calculated to obtain the percentage signal change values. The percentage signal change normalized by the values of the $EtCO_2$ change were also calculated. These percentage signal change values, normalized percentage signal change values, $EtCO_2$ change, and normalized *z*-map in three-dimensional space were averaged over all six subjects. Statistical analysis of percentage signal change values was performed by paired student's *t*-test. For the data processing and statistical analysis, the in-house software LIPSIA (Leipzig Image Processing and Statistical Interference Algorithms) was used (21).

RESULTS

All subjects performed the HV task well and without any adverse reactions or detectable gross head motion. Averaged $EtCO_2$ values during normal breathing were

Table 1
Mean Percentage (%) Signal Change, Mean %Signal Change/mmHg EtCO2 and *z*-score by Smaller ROI Setting

	SE-EPI			GRE-EPI		
	Mean %signal change (SD)	Mean %signal change/mmHg $EtCO_2$ (SD)	*z*-score	Mean %signal change (SD)	Mean %signal change/mmHg $EtCO_2$ (SD)	*z*-score
Hippocampus	−3.3 (2.7)	−0.134 (0.110)	13.0	−0.5 (1.6)	−0.026 (0.067)	2.2
Frontal	−1.5 (0.7)	−0.064 (0.027)	−10.0	−4.3 (4.0)	−0.175 (0.153)	−7.4
Cerebellum	−1.2 (1.0)	−0.049 (0.040)	−13.0	−0.6 (0.8)	−0.028 (0.034)	−11.0
Parietal	−1.7 (1.3)	−0.069 (0.043)	−6.4	−1.4 (0.9)	−0.057 (0.036)	−9.4
Occipital	−1.0 (0.8)	−0.040 (0.026)	−2.6	−1.1 (0.5)	−0.044 (0.015)	−11.0
Basal ganglia	−0.6 (0.5)	−0.027 (0.026)	−11.0	−1.4 (0.5)	−0.058 (0.028)	−7.0
White matter	0.1 (0.2)	0.006 (0.008)	−4.9	0.8 (0.3)	0.033 (0.018)	−10.0

z-scores shows that of the center voxel in the ROI.

41.0 (2.2) mmHg (standard deviation) for SE-EPI and 40.0 (2.3) for GE-EPI. Averaged $EtCO_2$ values during HV were 16.5 (4.2) for SE-EPI and 16.5 (2.4) for GE-EPI. All subject's $EtCO_2$ values were decreased by more than 16 mmHg. Mean $EtCO_2$ change was 24.5 (4.2) mmHg for GE-EPI and 23.5 (4.3) mmHg for SE-EPI.

Averaged percentage signal changes for the smaller ROI analysis and *z*-values from each region of the brain-regions examined are listed in Table 1. The results of the larger ROI analysis are shown in a graph (Fig. 2) and also numerically in Table 2. The percentage signal change values obtained from the two types of ROI showed comparable results. In GE-EPI, percentage signal change for both ROI types in the frontal cortex was larger than those of all other gray matter tissue ($P < 0.05$), and hippocampal percentage signal change for both ROI types was smaller than for all other gray matter tissue ($P < 0.05$). In SE-EPI, the percentage signal change in all cerebral cortex (gray matter tissue except hippocampal formation) was more uniform and there was no significant difference between each cortex. The percentage signal change for both ROI types in the frontal cortex was larger in GE-EPI than in SE-EPI ($P < 0.05$). In the parietal cortex, the signal change was slightly greater in SE-EPI than in GE-EPI, but this difference was not significant (Figs. 2 and 3). The signal change in the hippocampal formation could be appreciated in SE-EPI but was not apparent in GE-EPI, probably due to susceptibility artifact from the paranasal sinus. GE-EPI and SE-EPI images from this region are shown in Figure 4. Averaged percentage signal change of hippocampal formation in SE-EPI for both ROI types was larger than that of other gray matter tissue ($P < 0.05$). In white matter, a statistically significant signal increase for both ROI types was observed in GE-EPI. This white matter signal increase seemed to be located mostly in the frontal area in the watershed between the anterior and middle cerebral arteries (Fig. 3). This phenomenon was seen in all subjects.

In the occipital cortex, basal ganglia, and cerebellum, averaged percentage signal change by both ROI settings and normalized values by $EtCO_2$ was larger in GE-EPI than in SE-EPI, but the differences were not significant. On the *z*-maps (Fig. 3), the basal ganglia seemed to

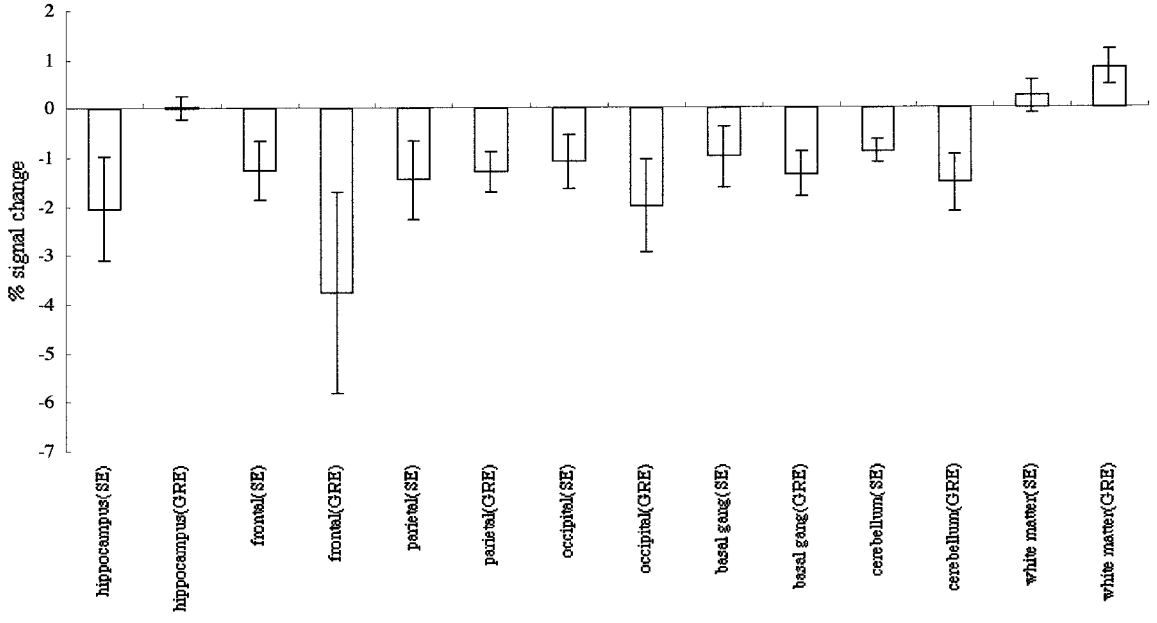

Figure 2. Mean percentage (%) signal changes for manually drawn ROIs during periodic HV task.

Table 2
Mean Percentage (%) Signal Change and Mean %Signal Change/mmHg EtCO2 by Larger ROI Setting

	SE-EPI		GRE-EPI	
	Mean %signal change (SD)	Mean %signal change/mmHg $EtCO_2$ (SD)	Mean %signal change (SD)	Mean %signal change/mmHg $EtCO_2$ (SD)
Hippocampus	−2.0 (1.1)	−0.080 (0.034)	0.0 (0.2)	0.001 (0.009)
Frontal	−1.3 (0.6)	−0.054 (0.032)	−3.8 (2.1)	−0.165 (0.099)
Cerebellum	−0.9 (0.2)	−0.037 (0.014)	−1.5 (0.6)	−0.066 (0.027)
Parietal	−1.5 (0.8)	−0.062 (0.035)	−1.3 (0.4)	−0.057 (0.024)
Occipital	−1.1 (0.6)	−0.046 (0.029)	−2.0 (0.9)	−0.086 (0.040)
Basal ganglia	−1.0 (0.6)	−0.043 (0.030)	−1.3 (0.5)	−0.059 (0.024)
White matter	0.3 (0.3)	0.012 (0.017)	0.8 (0.4)	0.036 (0.017)

show slightly more distinct vascular reactivity on SE-EPI than GE-EPI. The time courses of averaged percentage signal change in frontal cortex ROI and white matter ROI by larger ROI setting are shown both for SE-EPI and GE-EPI (Fig. 5).

DISCUSSION

Vascular reactivity to global cerebral stimulation, such as hypercapnia, hypocapnia, and pharmacological stress, has been investigated by positron emission tomography (PET) (1,22,23), near-infrared spectroscopy (24), and fMR imaging (4,6,25). Vascular reactivity has become of interest, because it can assist in the evaluation of activation-induced flow changes and pathologic changes in regional cerebral hemodynamics (24).

There are a number of methods by which a vasomotoric challenge can be achieved. Breath-holding has been employed as a simple and easy method for achieving hypercapnia in young healthy volunteers. However, to achieve a significant signal change, 30 seconds of breath-holding at expiration is necessary (6), which is not always possible for elderly or diseased subjects. Inhalation of CO_2 gas requires a specialized device, although it may cause less motion artifact compared to HV. Acetazolamide provides a pharmacological chal-

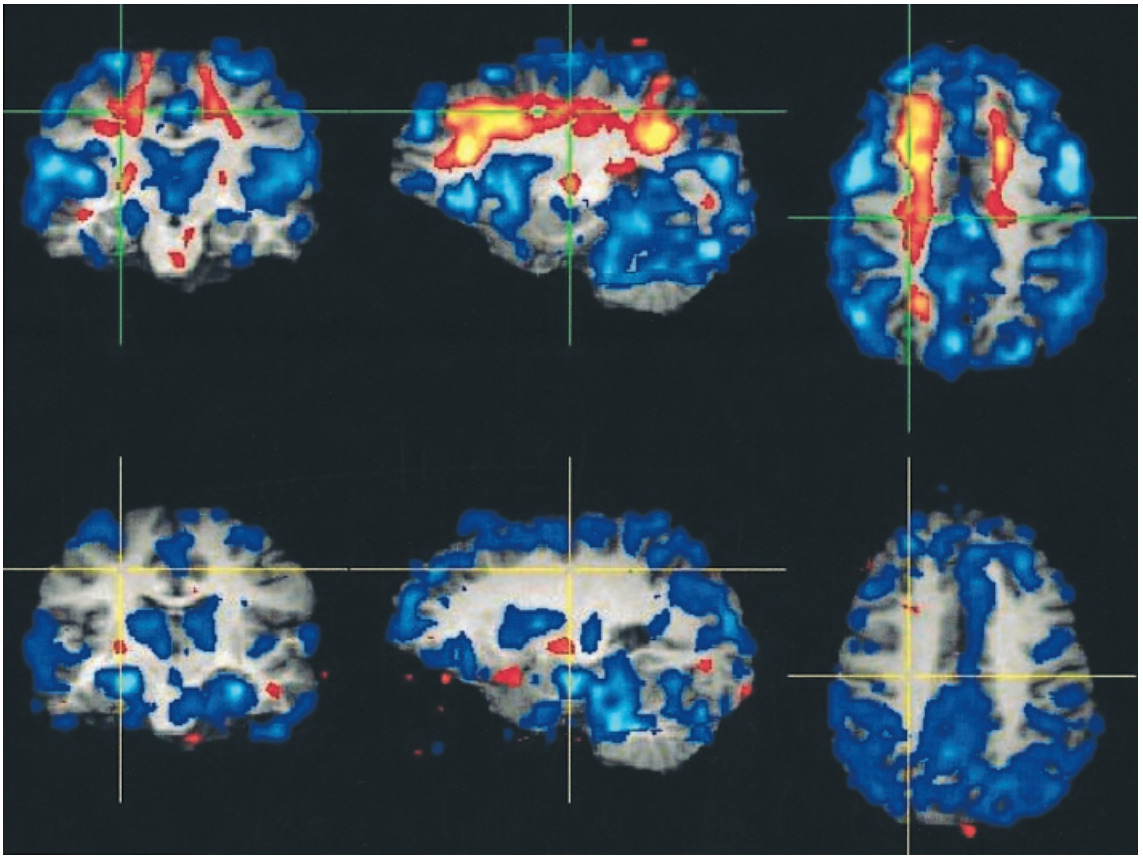

Figure 3. Averaged *z*-map of six subjects. Upper row shows *z*-maps from GE-EPI and lower row shows those from SE-EPI. Blue indicates the significant signal decrease and red indicates the significant signal increase. Note that hippocampal signal change is more conspicuous on SE-EPI. Frontal cortex dominance is less prominent on SE-EPI.

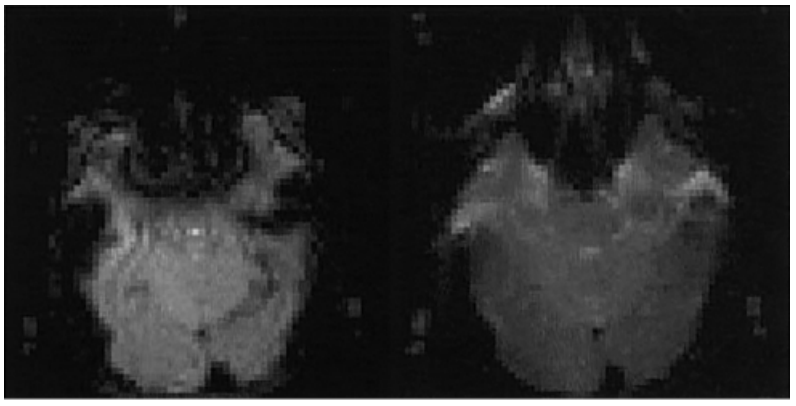

Figure 4. GE-EPI (**a**) and SE-EPI (**b**) images obtained in the region of the hippocampal formation. Note on GE-EPI (a) the hippocampal area is distorted and shows almost no signal due to severe susceptibility artifacts arising from the paranasal sinus.

lenge and is widely used as vasodilating agent; however, its use cannot be repeated in a short period and the true mechanism of its vasodilating action is still unknown (23). Ethanol ingestion is relatively easy, but it may affect not only the global cerebral blood flow, but also the neural activity itself (26,27). HV has been used as an easy and reliable task for the assessment of global cerebral vascular reactivity and it is believed that HV does not alter cerebral oxygen consumption except in extreme cases (4,28). The other advantages of HV over other pharmacological interventions are that it can be monitored non-invasively and regulated, it can cause rapid global cerebral blood flow (CBF) decrease (29), and it can be repeated at will. Furthermore, if the subject suffers an adverse reaction, HV can be terminated immediately. The disadvantage of HV is the risk of head motion, although it can be reduced by fixing the subject's head tightly and instructing the subject to not move.

The fMR signal depends on multiple physiological parameters, such as cerebral blood volume (CBV), CBF, and cerebral metabolic rate of oxygen ($CMRO_2$) (6,9,29–32). The physiological effect of HV is to reduce the $PaCO_2$ and then increase the perivascular pH. Increased perivascular pH induces marked vasoconstriction that results in a rapid reduction in CBF. To maintain the rate of oxidative energy metabolism during the blood flow reduction that occurs due to hypocapnia, an increased oxygen extraction fraction is necessary. This increases the deoxyhemoglobin concentration and reduces the BOLD-weighted MR signal intensity (3,4). However, except in extreme cases, HV does not alter cerebral oxygen consumption in healthy subjects (4,33). For a $PaCO_2$ decrease to 26 mmHg (hypocapnia), it is reported that CBF decreases by 30% and CBV decreases by 7.2% in healthy human subjects studied using radioisotopic methods (34). For these decreases in CBF and CBV, we can calculate percentage signal decreases according to the Balloon model for BOLD fMR imaging (31). The relative MR signal change is given by:

$$\frac{\Delta S}{S_0} = \frac{V_0}{\beta V_0 + 1 - V_0} \left\{ -(k_e(1 - V_0) + k_i\beta)\frac{\Delta C}{C_0} + (\beta - 1 - k_e(1 - V_0))\frac{\Delta V}{V_0} \right\}. \quad (1)$$

where S_0, V_0, and C_0 are the resting state values of the signal intensity, vascular volume, and deoxyhemoglobin concentration, respectively. The values of the parameters k_e, k_i, and β, for 1.5-T and 3-T are given in Table 3. In order to calculate $\Delta C/C_0$ from the ΔCBF value, we used the deoxyhemoglobin dilution model (32) or Fick's law. Then for a constant oxygen consumption, the relative change in the deoxyhemoglobin concentration is inversely proportional to that in blood flow, i.e., $\Delta C/C_0 = (1 + \Delta\text{CBF}/100)^{-1} - 1$. This yields $\Delta C/C_0 = +42\%$. If we take these values of $\Delta C/C_0$ and $\Delta V/V_0$ and use the parameters k_e, k_i, and β, Eq. [1] gives

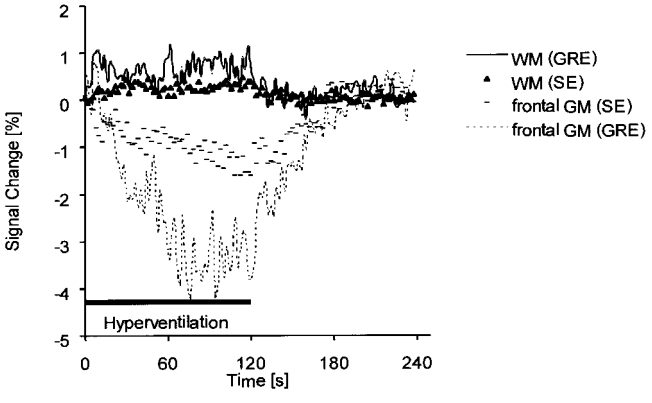

Figure 5. The time courses of mean percentage signal change of gray matter and white matter ($N = 6$) averaged over three rest and three HV periods. Note that the white matter signal stays near baseline during rest period and increases during the HV period. The response peak of gray matter seems to delayed compared to white matter.

Table 3
The Values of the Parameters k_e, k_i and β, for 1.5 T and 3 T for Balloon Model Simulation

	1.5 T (66 ms TE)	3 T (30 ms TE)[a]
k_I	0.94	1.71
k_e	4.62	4.19
β	1.79	0.59

[a]Measurement values obtained in the authors' laboratory.

$\Delta S/S = -4.7\%$ for an echo time of 66 msec at 1.5-T and $\Delta S/S = -3.8\%$ for an echo time of 30 msec at 3-T. In the present study, 1.1%–4.3% signal decrease was noted in cortical gray matter on GE-EPI. In the previous study at 1.5-T using GE-EPI (4), a 2.8%–5.3% signal decrease corresponds to their results for this degree of hypocapnia. These experimental values are comparable to the calculated values.

In the present study, the frontal cortex showed significantly larger signal change compared to other cortices on GE-EPI. This is consistent with the previous study (4). However, it is reported that the cerebellum and visual cortex have larger CBV values and higher capillary densities than the frontal cortex (6,35). In the present study, frontal lobe dominance in percentage signal change was less prominent in SE-EPI than GE-EPI. The $\Delta R2^*/\Delta R2$ ratio depends most strongly on the vessel radius and spin diffusion coefficient (36). At 2.0-T, it has been shown that CBF increase induced by hypercapnic stress in rats reduced R2* but did not change the apparent diffusion coefficient (ADC) of brain tissue (37). Thus, we can deduce that the frontal lobe dominance is mainly due to the contribution of vessels with larger diameter. The reason for the discrepancy between hypo- and hypercapnia is still not clear. The regional cerebrovascular reactivities to hypo- and hypercapnia might differ. A breath-holding study using the same methods as the present study would be of interest. The one possible cause for the discrepancy between hypo- and hypercapnia may be the degree of head motion, although we could not see the detectable gross motion and we could not see the frontal dominance in SE-EPI. As we used a relatively short repetition time of two seconds, slight sub-voxel head motion in the *z*-direction might have caused the slight signal fluctuation. The study with three-dimensional thick slab EPI may be interesting for future study to reduce the risk of signal modulation by slight head motion in the *z*-direction.

The frontal cortices, especially their medial aspect, are sometimes influenced by field inhomogeneities caused by paranasal sinuses. However, in this study, ROIs were set on relatively upper slices (Fig. 1); thus, the effect of paranasal sinuses are thought to be small.

At 1.5-T, SE-EPI had significantly lower BOLD signal changes than GE-EPI (7,8), and as mentioned above, the two methods had different sensitivities to various vascular structures (9). In the present study at 3-T, the largest percentage signal decrease in SE-EPI was found in the hippocampal formation. This is compatible with a previous report in rats that hippocampal formation was most susceptible to hypocapnia and showed significantly greater signal decreases than other parts of the brain (38). Vascular reactivity and blood flow in the hippocampal formation is important for the assessment of transient global amnesia (39), Alzheimer disease (40), and other pathologies. The results of this study suggest that the combined use of SE-EPI and HV at 3-T provides an easy vascular reactivity test for the hippocampal formation, which would have been impossible with GE-EPI due to severe susceptibility artifacts from the paranasal sinus.

The signal increase in white matter due to HV was an unexpected result. It has been reported that white matter signal change is delayed by three seconds compared to gray matter in a hypercapnia study (20). In the current study, as shown in Figure 5, the peak of gray matter signal change due to hypocapnia was delayed compared to that of white matter. This also suggests a difference in physiological response to hypo- and hypercapnia. However, the two minute HV duration employed here was so long that it is inconceivable that the white matter change should be in antiphase to the gray matter change. Furthermore, the white matter signal during the rest period stayed near baseline, which is inconsistent with a phase shift. We have excluded the possibility of white matter signal alteration during the preprocessing period by measuring the signal from a ROI on non-preprocessed raw data, as well as preprocessed data. A partial volume averaging artifact can be excluded by the large area of significant signal increase in white matter. We are convinced that the slight white matter signal increase during HV is not artifactual; however, we are at present unable to offer a physiological explanation for this phenomen. One possibility would be if there was a rapid increase in the resistance to blood flow in gray matter that could cause a transient blood increase in white matter. It should be emphasized that while this would offer a mechanistic explanation for the effect, it is not corroborated with any physiological evidence. The distribution of the white matter signal increase seems to correspond to the watershed between the anterior and middle cerebral artery; it is possible that this region may have a different vascular reactivity.

In the basal ganglia, the averaged percentage signal change by both ROI settings and normalized values by $EtCO_2$ was larger in GE-EPI than in SE-EPI, although the differences were not significant. On the *z*-maps, the basal ganglia seemed to show slightly more distinct vascular reactivity on SE-EPI than GE-EPI. The *z*-map showed the degree of correlation to the task design, not the degree of vascular response itself. This may be the cause of the discrepancy between percentage signal change and *z*-maps. The breathing motion itself is reported to cause the magnetic field alteration and results in the signal intensity modification by $\pm 1\%$ and the pseudo-motion artifact by 0.1 pixel in phase encoding direction (41). These artifacts by breathing motion should also be evaluated in future studies.

In conclusion, we consider the HV task combined with SE-EPI at 3-T to be a robust and reproducible method for evaluating cerebral vascular reactivity. It is of interest to investigate whether HV with SE-EPI is feasible even in the elderly and patient populations. If so, this method may find utility not only in basic scientific investigations such as that reported here, but also in clinical application.

REFERENCES

1. Bednarczyk EM, Rutherford WF, Leisure GP, et al. Hyperventilation-induced reduction in cerebral blood flow: assessment by positron emission tomography. Ann Pharmacother 1990;24:456–460.

2. Toft PB, Leth H, Lou HC, Pryds O, Peitersen B, Henriksen O. Local vascular CO2 reactivity in the infant brain assessed by functional MRI. Pediatr Radiol 1995;25:420–424.
3. Posse S, Dager SR, Richards TL, et al. In vivo measurement of regional brain metabolic response to hyperventilation using magnetic resonance: proton echo planar spectroscopic imaging (PEPSI). Magn Reson Med 1997;37:858–865.
4. Posse S, Olthoff U, Weckesser M, Jancke L, Muller-Gartner HW, Dager SR. Regional dynamic signal changes during controlled hyperventilation assessed with blood oxygen level-dependent functional MR imaging. AJNR Am J Neuroradiol 1997;18:1763–1770.
5. Tsuda Y, Hartmann A. Changes in hyperfrontality of cerebral blood flow and carbon dioxide reactivity with age. Stroke 1989;20:1667–1673.
6. Kastrup A, Kruger G, Glover GH, Neumann-Haefelin T, Moseley ME. Regional variability of cerebral blood oxygenation response to hypercapnia. Neuroimage 1999;10:675–681.
7. Bandettini PA, Wong EC, Jesmanowicz A, Hinks RS, Hyde JS. Spin-echo and gradient-echo EPI of human brain activation using BOLD contrast: a comparative study at 1.5 T. NMR Biomed 1994; 7:12–20.
8. Lowe MJ, Lurito JT, Mathews VP, Phillips MD, Hutchins GD. Quantitative comparison of functional contrast from BOLD-weighted spin-echo and gradient-echo echoplanar imaging at 1.5 Tesla and H2 15O PET in the whole brain. J Cereb Blood Flow Metab 2000; 20:1331–1340.
9. Boxerman JL, Bandettini PA, Kwong KK, et al. The intravascular contribution to fMRI signal change: Monte Carlo modeling and diffusion-weighted studies in vivo. Magn Reson Med 1995;34:4–10.
10. Constable RT, Kennan RP, Puce A, McCarthy G, Gore JC. Functional NMR imaging using fast spin echo at 1.5 T. Magn Reson Med 1994;31:686–690.
11. Hoogenraad FG, Pouwels PJ, Hofman MB, Reichenbach JR, Sprenger M, Haacke EM. Quantitative differentiation between BOLD models in fMRI. Magn Reson Med 2001;45:233–246.
12. Oja JM, Gillen J, Kauppinen RA, Kraut M, van Zijl PC. Venous blood effects in spin-echo fMRI of human brain. Magn Reson Med 1999;42:617–626.
13. Lee SP, Silva AC, Ugurbil K, Kim SG. Diffusion-weighted spin-echo fMRI at 9.4 T: microvascular/tissue contribution to BOLD signal changes. Magn Reson Med 1999;42:919–928.
14. Ugurbil K, Garwood M, Ellermann J, et al. Imaging at high magnetic fields: initial experiences at 4 T. Magn Reson Q 1993;9:259–277.
15. Norris DG. Reduced power multislice MDEFT imaging. J Magn Reson Imaging 2000;11:445–451.
16. Lee JH, Garwood M, Menon R, et al. High contrast and fast three-dimensional magnetic resonance imaging at high fields. Magn Reson Med 1995;34:308–312.
17. Friston KJ. Statistical parametric maps in functional imaging: a general linear approach. Human Brain Mapping 1994;2:189–210.
18. Bosch V. Statistical analysis of multi-subject fMRI data: the assessment of focal activations. J Magn Reson Imaging 2000;11:61–64.
19. Talairach J, Tournoux P. Co-planar stereotaxic atlas of human brain. New York: Thieme; 1988.
20. Rostrup E, Law I, Blinkenberg M, et al. Regional differences in the CBF and BOLD responses to hypercapnia: a combined PET and fMRI study. Neuroimage 2000;11:87–97.
21. Lohmann G, Mueller K, Bosch V, et al. LIPSIA-leipzig image processing and statistical interference alogorithms. Technical report. Leipzig: Max Planc Institute of Cognitive Neuroscience; 2000.
22. De Reuck J, Decoo D, Hasenbroekx MC, et al. Acetazolamide vasoreactivity in vascular dementia: a positron emission tomographic study. Eur Neurol 1999;41:31–36.
23. Inao S, Tadokoro M, Nishino M, et al. Neural activation of the brain with hemodynamic insufficiency. J Cereb Blood Flow Metab 1998; 18:960–967.
24. Terborg C, Gora F, Weiller C, Rother J. Reduced vasomotor reactivity in cerebral microangiopathy: a study with near-infrared spectroscopy and transcranial Doppler sonography. Stroke 2000;31: 924–929.
25. Gollub RL, Breiter HC, Kantor H, et al. Cocaine decreases cortical cerebral blood flow but does not obscure regional activation in functional magnetic resonance imaging in human subjects. J Cereb Blood Flow Metab 1998;18:724–734.
26. Levin JM, Ross MH, Mendelson JH, et al. Reduction in BOLD fMRI response to primary visual stimulation following alcohol ingestion. Psychiatry Res 1998;82:135–146.
27. Seifritz E, Bilecen D, Hanggi D, et al. Effect of ethanol on BOLD response to acoustic stimulation: implications for neuropharmacological fMRI. Psychiatry Res 2000;99:1–13.
28. van Rijen PC, Luyten PR, van der Sprenkel JW, et al. 1H and 31P NMR measurement of cerebral lactate, high-energy phosphate levels, and pH in humans during voluntary hyperventilation: associated EEG, capnographic, and Doppler findings. Magn Reson Med 1989;10:182–193.
29. Weckesser M, Posse S, Olthoff U, Kemna L, Dager S, Muller-Gartner HW. Functional imaging of the visual cortex with bold-contrast MRI: hyperventilation decreases signal response. Magn Reson Med 1999;41:213–216.
30. Ogawa S, Menon RS, Tank DW, et al. Functional brain mapping by blood oxygenation level-dependent contrast magnetic resonance imaging: a comparison of signal characteristics with a biophysical model. Biophys J 1993;64:803–812.
31. Buxton RB, Wong EC, Frank LR. Dynamics of blood flow and oxygenation changes during brain activation: the balloon model. Magn Reson Med 1998;39:855–864.
32. Hoge RD, Atkinson J, Gill B, Crelie GR, Marrett S, Pike GB. Investigation of BOLD signal dependence on cerebral blood flow and oxygen consumption: the deoxyhemoglobin dilution model. Magn Reson Med 1999;42:849–863.
33. van Rijen PC, Luyten PR, van der Sprenkel JW, et al. 1H and 31P NMR measurement of cerebral lactate, high-energy phosphate levels, and pH in humans during voluntary hyperventilation: associated EEG, capnographic, and Doppler findings. Magn Reson Med 1989;10:182–193.
34. Fortune JB, Feustel PJ, deLuna C, Graca L, Hasselbarth J, Kupinski AM. Cerebral blood flow and blood volume in response to O2 and CO2 changes in normal humans. J Trauma 1995;39:463–471; discussion 471–472.
35. Perlmutter JS, Powers WJ, Herscovitch P, Fox PT, Raichle ME. Regional asymmetries of cerebral blood flow, blood volume, and oxygen utilization and extraction in normal subjects. J Cereb Blood Flow Metab 1987;7:64–67.
36. Bandettini PA, Wong EC. Effects of biophysical and physiological-parameters on brain activation-induced R2* and R2 changes – simulations using deterministic diffusion-model. Int J Imag Sys Tech 1995;6:133–152.
37. Graham GD, Zhong J, Petroff OA, Constable RT, Prichard JW, Gore JC. BOLD MRI monitoring of changes in cerebral perfusion induced by acetazolamide and hypercarbia in the rat. Magn Reson Med 1994;31:557–560.
38. Waaben J, Husum B, Hansen AJ, Gjedde A. Regional cerebral blood flow and glucose utilization during hypocapnia and adenosine-induced hypotension in the rat. Anesthesiology 1989;70:299–304.
39. Takeuchi R, Yonekura Y, Matsuda H, et al. Resting and acetazolamide-challenged technetium-99m-ECD SPECT in transient global amnesia. J Nucl Med 1998;39:1360–1362.
40. Julin P, Lindqvist J, Svensson L, Slomka P, Wahlund LO. MRI-guided SPECT measurements of medial temporal lobe blood flow in Alzheimer's disease. J Nucl Med 1997;38:914–919.
41. Raj D, Paley DP, Anderson AW, Kennan RP, Gore JC. A model for susceptibility artifacts from respiration in functional echo-planar magnetic resonance imaging. Phys Med Biol 2000;45:3809–3820.